J. Chosun Natural Sci.
Vol. 9, No. 3 (2016) pp. 177 – 184
http://dx.doi.org/10.13160/ricns.2016.9.3.177

Comparative Molecular Similarity Indices Analysis of CXCR-2 Inhibitors

Sathya. B†

Abstract

CXC chemokine receptor 2 (CXCR2) is a prominent chemokine receptor on neutrophils and it regulates the neutrophilic inflammation in the lung diseases. CXCR2 antagonist may reduce the neutrophil chemotaxis and alter the inflammatory response. Hence, in the present study, ligand based Comparative Molecular Similar Indices Analysis (CoMSIA) was performed on a series of CXCR2 antagonist named pyrimidine-5-carbonitrile-6-alkyl derivatives. The optimum CoMSIA model was obtained with statistically significant cross-validated coefficients (q^2) of 0.582 and conventional coefficients (r^2) of 0.987 with steric, electrostatic, hydrophobic, donor and acceptor fields. The contour maps suggest the important structural modifications and this study can be used to guide the development of potent CXCR2 antagonist.

Keywords: CXCR2; CoMSIA

1. Introduction

Chemokines are small 8-10 kDa which act through G-protein-coupled receptors (GPCRs) to regulate a variety of effects, including cell migration and inflammatory events. Chemokines have long been implicated in the initiation and amplification of inflammatory responses by their role in leukocyte chemotaxis[1,2]. They are currently seven known CXCR receptor found in mammals named CXCR1-CXCR7. CXCR2 (also called CD182, IL8) is found on many cells including leukocytes, endothelial and epithelial cells[3,4] and plays a critical role in the regulation of neutrophil homeostasis[5]. CXCR2 receptor may have a broad functional role in number of acute and chronic diseases and can be released from a number of inflammatory and structural cell types. CXCR2 is also expressed by neutrophil precursors in the bone marrow that can be released during systemic inflammation. It plays an important role in asthma, chronic obstructive pulmonary disease (COPD) and fibrotic pulmonary disorders[6-8]. It was found that neutrophilic inflammation in the lung diseases is found to be largely regulated through CXCR2[2,9]. In some cancers, such as prostate cancer, CXCR2 is expressed by early premalignant cells, but downregulated during tumor progression. Therefore blockade of CXCR2 substantially reduces tissue damage, leukocyte recruitment, and mortality. An antagonist of CXCR2 reduces neutrophilic chemotaxis and may alter the airway inflammation. To date, there are no CXCR2 receptor antagonists approved for use in humans. However, several pharmaceutical companies have disclosed CXCR2 antagonists and amongst these, navarixin and AZD-5069 are noteworthy.

When 3D structure of the macromolecular target is not available 3D-QSAR is the prominent computational means to support chemistry within drug design projects[10] and is demonstrated in many studies[11-14]. Hence, in the present 3D QSAR method, CoMSIA model was generated utilizing pyrimidine-5-carbonitrile-6-alkyl derivatives as CXCR2 antagonist. The five CoMSIA models were developed with the different combinations of steric, electrostatic, hydrophobic, donor and acceptor fields. The CoMSIA model was graphically interpreted by a field contribution map which provides guidelines for the design of new compounds with enhanced activity and specificity.

Department of Genetic Engineering, School of Bioengineering, SRM University, SRM Nagar, Kattankulathur, Chennai 603203, India

†Corresponding author : sathyainfo26@gmail.com
(Received: July 21, 2016, Revised: September 18, 2016, Accepted: September 25, 2016)

2. Materials and Methods

2.1. Data set

The structure and biological activities of 26 compounds named pyrimidine-5-carbonitrile-6-alkyl derivatives were taken from the literature[15]. Biological activities i.e. IC_{50} of these compounds was converted into pIC_{50} ($-logIC_{50}$) in order to use in CoMSIA analysis as the dependent variable. The dataset (26 compounds) was segregated into test (5 compounds) and training set

Table 1. Structures and biological activities (pIC_{50}) of CXCR2 inhibitors

Cmpd no	Structure	pIC_{50} values	Cmpd no	Structure	pIC_{50} values
1	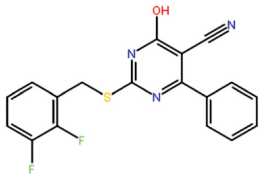	5.432	14	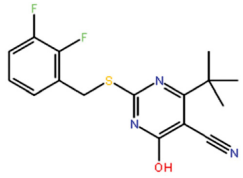	5.432
2	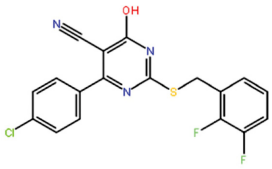	5.130	15	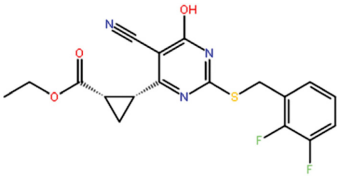	5.824
3	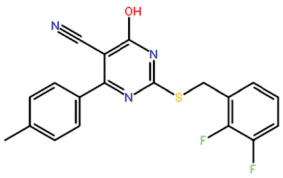	5.854	16	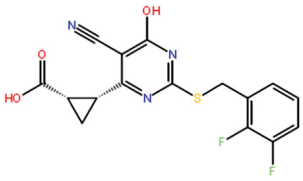	8.000
4	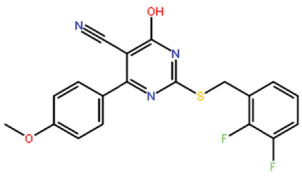	6.148	17	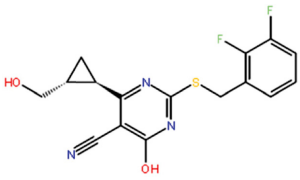	8.222
5	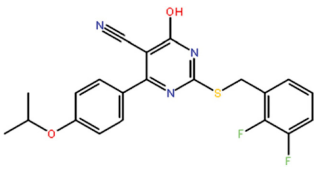	5.795	18	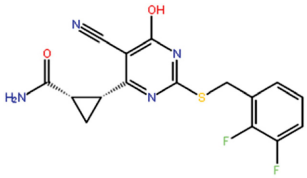	8.155
6	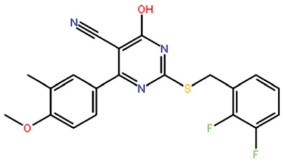	5.337	19	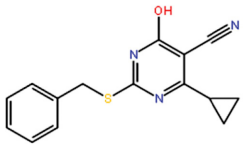	6.292
7	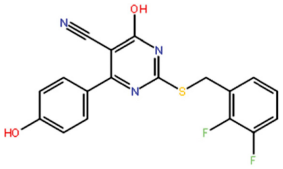	6.107	20	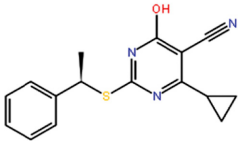	5.318

Table 1. Continued

Cmpd no	Structure	pIC_{50} values	Cmpd no	Structure	pIC_{50} values
8	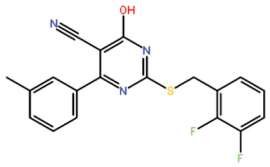	5.327	21	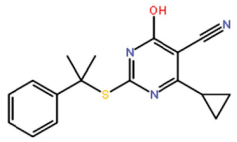	5.193
9	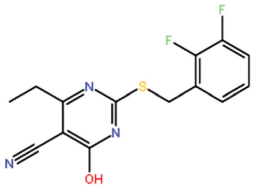	5.366	22	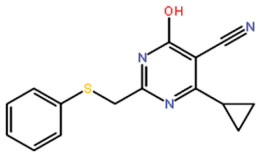	4.522
10	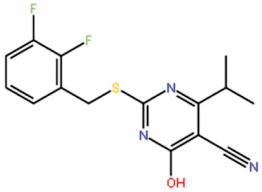	6.045	23	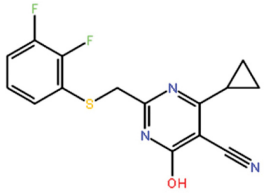	5.000
11	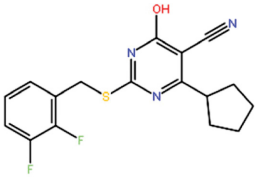	5.309	24	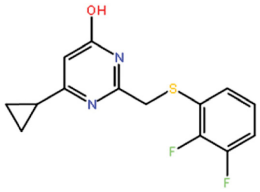	6.495
12	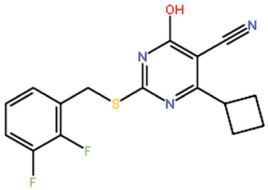	5.769	25	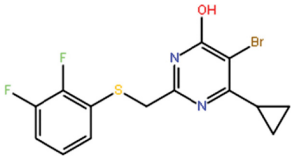	5.854
13	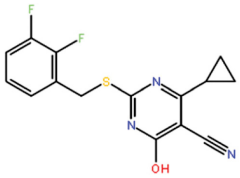	6.853	26	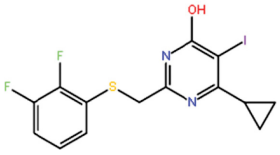	5.495

(21 compounds). The training and test sets were classified to ensure that both sets could completely cover the whole range of biological activity and structural diversity. The structures and their activity pIC_{50} values are displayed in Table 1.

2.2. Structural Alignment

The structure of 26 CXCR2 inhibitors was drawn using sketch molecule function in SYBYL-X2.1[16] version and its partial atomic charge were assigned using Gasteiger-Huckel method. The highly active molecule (compound 17) among the dataset was selected as template and its bioactive conformation was searched through systematic search analysis. The lowest energy conformer of the highly active molecule was assumed to be the bioactive conformation and it was used to

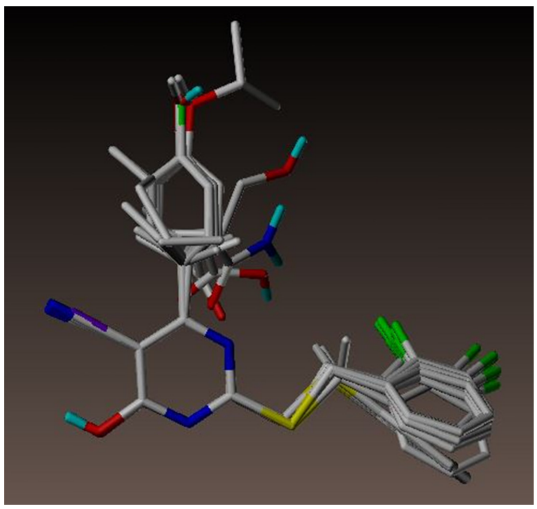

Fig. 1. Superimposed structure of all molecules based on atom by atom matching alignment.

align all the compounds. The aligned molecules were subsequently used for CoMSIA analysis. The alignment of all molecules is represented in Fig. 1.

2.3. CoMSIA Analysis

CoMSIA has better ability to visualize and interpret the field contributions such as steric, electrostatic, hydrophobic, hydrogen bond donor and acceptor fields. These five physico-chemical properties were evaluated within a 3D grid using a common probe atom[17]. CoMSIA similarity indices for molecule *j* with atom *i* at a grid point q were calculated using the following equation:

$$A_{F,K}^{q} = -\sum_{i=1}^{n} W\,probe, k W_{ik} e^{-ar_{iq}^{2}}$$

where *k* represents the following physicochemical properties: steric, electrostatic, hydrophobic, H-bond donor, and H-bond acceptor. Gaussian-type distance dependence with default attenuation factor of 0.3 was assumed in the CoMSIA calculation.

2.4. PLS Analysis and Predictive Correlation Coefficient

In 3D-QSAR, CoMSIA descriptors were used as independent variables and pIC_{50} values were used as the dependent variable. Partial least squares (PLS) method[18] was used to explore a linear correlation between the CoMSIA fields and the biological activity values. For the calculation of steric and electrostatic fields, the cutoff values were set to 30 kcal⁄mol, and all fields were scaled by the default options. Leave one out cross validation (LOO)[19] was used to perform the regression analysis. The cross-validation correlation coefficient (q^2) that resulted in a minimal number of components and the lowest cross-validated standard error of estimate was considered for further analysis and calculated using the formula:

$$q^2 = 1 - \frac{\sum_{\gamma}(\gamma_{pred} - \gamma_{actual})^2}{\sum_{\gamma}(\gamma_{actual} - \gamma_{mean})^2}$$

where γpred, γactual, and γmean are the predicted, actual, and mean values of the target property (pIC_{50}), respectively. CoMSIA results were then graphically interpreted by field contribution maps.

To derive the predictive power of 3D-QSAR models, test set molecules which were excluded during model development was used. The model derived from training set was used to predict the activity of the test set. The following formula was used to determine the predictive correlation coefficient r^2_{pred} of the developed model.

$$r_{pred}^2 = \left(\frac{SD - PRESS}{SD}\right)$$

where, SD is defined as the sum of the square deviation between the biological activity of the test set compounds and the mean activity of the training set molecules and PRESS is the sum of the squared deviation between the predicted and actual activity of the test set molecules.

3. Results and Discussions

In the present work, we have generated CoMSIA model for CXCR2 inhibitors (pyrimidine-5-carbonitrile-6-alkyl derivatives). Statistical values like q^2, r^2, SEE, F value and r^2_{pred} were calculated for different fields. The best predictions were obtained for CoMSIA model (q^2 = 0.582, r^2 = 0.987).

Table 2. Statistical results of CoMSIA models

PLS statistics	Model 1	Model 2	Model 3	Model 4	Model 5
q^2	0.485	0.563	0.628	0.473	0.582
N	3	6	6	6	6
r^2	0.947	0.990	0.985	0.985	0.987
SEE	0.231	0.114	0.140	0.136	0.127
F-value	89.959	193.353	127.394	134.979	154.549
r^2_{pred}	0.525	0.711	0.695	0.587	0.765
Field contribution					
Steric	0.209	0.143	0.161	0.186	0.095
Electrostatic	0.791	0.555	0.579	0.545	0.404
Hydrophobic	-	0.302	-	-	0.190
Donor	-	-	0.260	-	0.167
Acceptor	-	-	-	0.269	0.142

q^2= cross-validated correlation coefficient; N= number of statistical components; r^2= non-cross validated correlation coefficient; SEE=standard estimated error; F=Fisher value; $r^2_{predictive}$= predictive correlation coefficient for test set.

3.1. CoMSIA Statistical Analysis

CoMSIA analysis was carried out to evaluate the steric, electrostatic, hydrophobic, donor and acceptor properties. Many different CoMSIA models were generated with different combinations of training and test set and the best model was selected based on their statistical results. The statistical result of CoMSIA models was given in Table 2. For the selected model leave one out analysis gave the cross-validated q^2 of 0.582 with six components and non-cross-validated PLS analysis resulted in a correlation coefficient r^2 of 0.987, F = 154.549, and an estimated standard error of 0.127. The contribution of the steric, electrostatic, hydrophobic, donor and acceptor fields were 10%, 40%, 20&, 16% and 14% respectively. This indicates the electrostatic field contributes more than other fields. Good correlation was observed between the predicted and experimental activities indicating the goodness of the model. Predicted, experimental activities (pIC_{50}) and their residual values of all inhibitors are shown in Table 3.

3.2. Mapping of CoMSIA Contour Map

The CoMSIA contour map was generated for the best model and it is shown in Fig. 2. This shows the regions where steric, electrostatic, hydrophobic, H-bond donor and acceptor features of the different molecules contained in the training set leads to increase or decrease in the activity. In Fig. 2(a) steric contour has green contour which indicates region where a bulky group

Table 3. Predicted activities of CoMSIA model compared with the experimental pIC_{50} values

S.No	Actual pIC_{50}	Predicted pIC_{50}	Residual
1.	5.432	5.649	-0.218
2.	5.130	5.755	-0.625
3.	5.854	5.789	0.065
4.	6.148	5.917	0.231
5.	5.795	5.762	0.033
6.	5.337	5.485	0.148
7.	6.107	6.085	0.022
8.	5.327	5.200	0.127
9.	5.366	6.154	-0.788
10.	6.045	6.064	-0.019
11.	5.309	5.417	-0.108
12.	5.769	5.782	-0.013
13.	6.853	5.996	0.857
14.	5.432	5.497	-0.066
15.	5.824	5.785	0.038
16.	8.000	8.029	-0.029
17.	8.222	8.178	0.048
18.	8.155	7.693	0.046
19.	6.292	6.165	0.127
20.	5.318	5.552	-0.234
21.	5.193	5.115	0.078
22.	4.522	4.506	0.016
23.	5.000	4.902	0.098
24.	6.495	6.584	-0.089
25.	5.854	5.822	0.032
26.	5.495	5.728	-0.233

increases the activity and yellow contours indicates a bulky group decreases the activity. The green steric contour explains the presence of bulky cyclopropyl ring attached to pyrimidine ring and the bulky benzyl attached to sulfur makes the compound potent with higher activity. Hence bulky groups in those positions are favorable. We have observed that the compounds which does not have bulky cyclopropyl ring have lower activity. The electrostatic contour in Fig. 2(b) shows blue and red contour indicating the regions where an electropositive and electronegative group increases the activity. The red colored region indicates the electron-

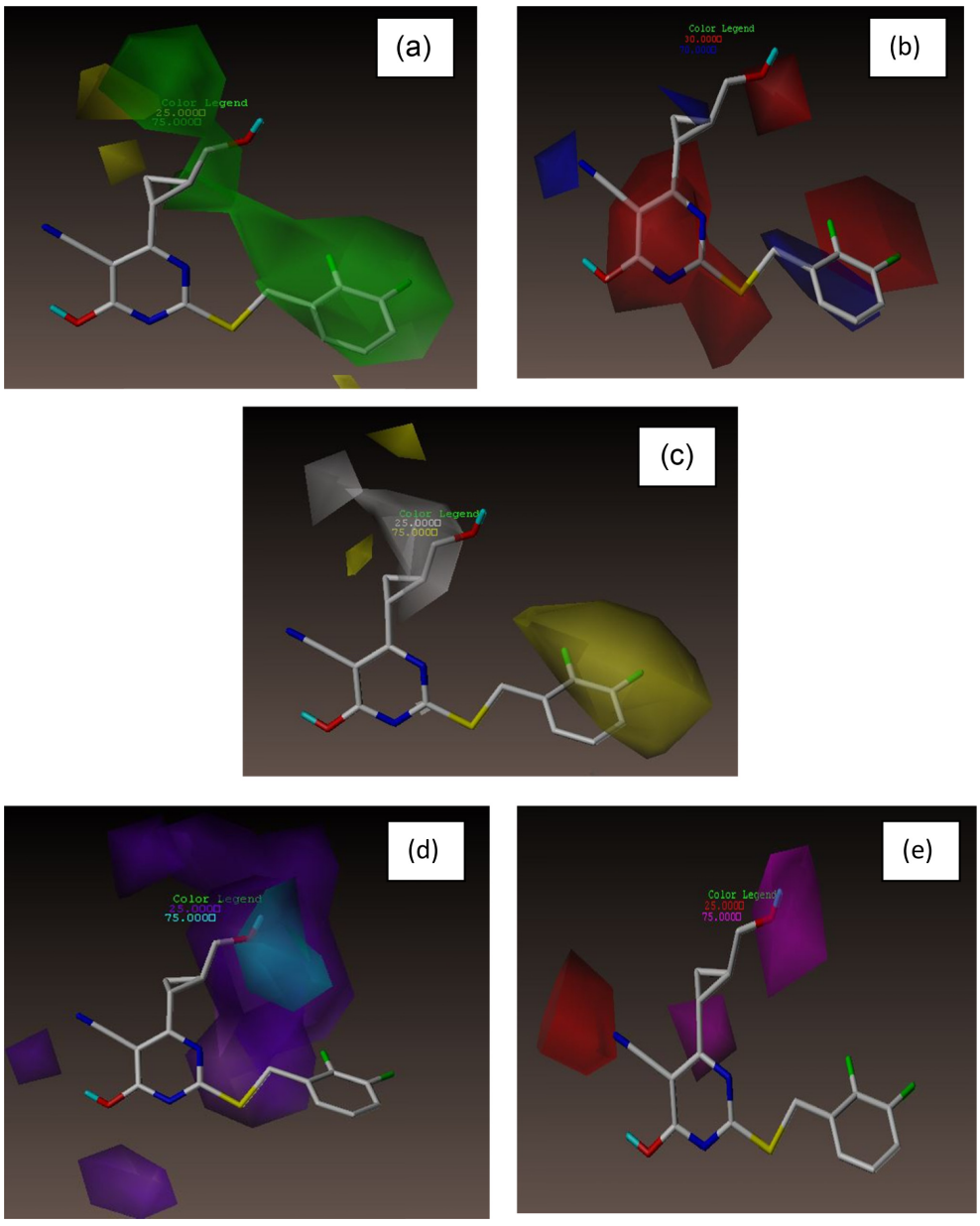

Fig. 2. CoMSIA contour maps for compound 17. (a) Steric contour map (b) Electrostatic contour map(c) Hydrophobic contour map (d) H-bond donor contour map (e) H-bond acceptor contour map.

egative atom in ortho and meta position of benzyl attached to sulfur is favorable in increasing the activity. Fig. 2(c) represents the hydrophobic contour map, where yellow indicates the region where the hydrophobic substitutions are favorable for activity and white contour indicates the disfavored region for inhibitory activity. The presence of hydrophobic atoms around benzyl ring and the presence of hydrophilic atoms around cyclopropyl ring are highly favorable in enhancing the activity. In Fig. 2(d), H-bond donor contour depicts the cyan indicating region where hydrogen bond donor substituents enhance activity and purple indicating hydrogen bond donor substituents reduces activity. H-bond acceptor contour in Fig. 2(e) represents the magenta and red color which indicates where hydrogen bond acceptor group increases and decreases the activity. The presence of hydrogen bond donor and acceptor groups in cyclopropyl ring could contribute to the inhibitory activity of CXCR2 inhibitors.

4. Conclusion

The CoMSIA contour map gives valuable information to understand 3D-QSAR relationships between the structures and their biological activity. The contour maps suggest the presence of bulky and hydrogen bond donor and acceptor group in the cyclopropyl ring and bulky electronegative atoms in benzyl ring could improve the activity of these compounds. The information obtained from 3D-QSAR study could be useful for improving and predicting the activities of new CXCR2 antagonists.

References

[1] M. Uguccioni, M. D'Apuzzo, M. Loetscher, B. Dewald, and M. Baggiolini, "Actions of the chemotactic cytokines MCP-1, MCP-2, MCP-3, RANTES, MIP-1 alpha and MIP-1 beta on human monocytes", Eur. J. Immunol., Vol. 25, pp. 64-68, 1995.

[2] R. W. Chapman, J. E. Phillips, R. W. Hipkin, A. K. Curran, D. Lundell, and J. S. Fine, "CXCR2 antagonists for the treatment of pulmonary disease", Pharmacol. Therapeut., Vol. 212, pp. 55-68, 2009.

[3] J. Reutershan, A. Basit, E. V. Galkina, and K. Ley, "Sequential recruitment of neutrophils into lung and bronchoalveolar lavage fluid in LPS-induced lung injury", Am. J. Physiol-Lung C., Vol. 289, pp. L807-L815, 2005.

[4] S. L. Traves, S. J. Smith, P. J. Barnes, and L. E. Donnelly, "Specific CXC but not CC chemokines cause elevated monocyte migration in COPD: a role for CXCR2", J. Leukocyte. Biol., Vol. 76, pp. 441-450, 2004.

[5] K. J.Eash, A. M. Greenbaum, P. K. Gopalan, and D. C. Link, "CXCR2 and CXCR4 antagonistically regulate neutrophil trafficking from murine bone marrow", J. Clin. Invest., Vol. 120, pp. 2423-2431, 2010.

[6] R. A. Pauwels and K. F. Rabe, "Burden and clinical features of chronic obstructive pulmonary disease (COPD)", Lancet, Vol. 364, pp. 613-620, 2004.

[7] E. H. Bel, A. Sousa, L. Fleming, A. Bush, K. F Chung, J. Versnel, A. H. Wagener, S. S. Wagers, P. J. Sterk, and C. H. Compton, "Diagnosis and definition of severe refractory asthma: an international consensus statement from the Innovative Medicine Initiative (IMI)", Thorax, 2010.

[8] P. Anderson, "Emerging therapies in cystic fibrosis", Ther. Adv. Respir. Dis., Vol. 4, pp. 177-185, 2010.

[9] P. M. Murphy, "Neutrophil receptors for interleukin-8 and related CXC chemokines", Semin. Hematol., Vol. 34, pp. 311-318, 1997.

[10] W. Sippl, "3D-QSAR – Applications, recent advances, and limitations", in Recent Advances in QSAR Studies: Methods and Applications, Heidelberg: Springer, 2010

[11] B. Sathya and M. Thirumurthy, "Pharmacophore based comparative molecular field analysis of CRTh2 antagonists", J. Chosun Natural Sci., Vol. 8, pp. 89-98, 2015.

[12] B. Sathya and M. Thirumurthy, "Comparative molecular field analysis of caspase-3 inhibitors", J. Chosun Natural Sci., Vol. 7, pp. 166-172, 2014.

[13] M. Thirumurthy, "Modeling aided lead design of FAK inhibitors", J. Chosun Natural Sci., Vol. 4, pp. 266-272, 2011.

[14] M. Thirumurthy, "3D-QSAR studies of 3,5-disubstituted quinolines inhibitors of c-Jun N-terminal kinase-3", J. Chosun Natural Sci., Vol. 4, pp. 216-221, 2011.

[15] D. W. Porter , M. Bradley, Z. Brown, S. J. Charlton, B. Cox, P. Hunt, D. Janus, S. Lewis, P. Oakley, D. O'Connor, J. Reilly, N. Smith, and N. J. Press, "The discovery of potent, orally bioavailable pyrimidine-5-carbonitrile-6-alkyl CXCR2 receptor antagonists", Bioorg. Med. Chem. Lett., Vol. 24, pp. 3285–3290, 2014.

[16] SYBYL Software, Version X 2.0., 2006, Tripos Associates Inc, St. Louis, USA.
[17] G. Klebe, U. Abraham, and T. Mietzner, "Molecular similarity indices in a comparative analysis (CoMSIA) of drug molecules to correlate and predict their biological activity", J. Med. Chem., Vol. 37, pp. 4130-4146, 1994.
[18] S. Wold, A. Ruhe, H. Wold, and W. J. Dunn, "The collinearity problem in linear-regression- the partial least squares (PLS) approach to generalized inverses", SIAM Journal on Scientific and Statistical Computing, Vol. 5, pp. 735-743, 1984.
[19] S. Wold, "Cross-validatory estimation of the number of components in factor and principal component model", Technometrics, Vol. 20, pp. 397-405, 1978.